NeuroImage: Clinical 25 (2020) 102166

Contents lists available at ScienceDirect

NeuroImage: Clinical

journal homepage: www.elsevier.com/locate/ynicl

A 7 Tesla fMRI investigation of human tinnitus percept in cortical and subcortical auditory areas

Eva Berlot[a,b], Remo Arts[c], Jasper Smit[d,e], Erwin George[f], Omer Faruk Gulban[a], Michelle Moerel[a,g], Robert Stokroos[h], Elia Formisano[a,g], Federico De Martino[a,i,*]

[a] Department of Cognitive Neuroscience, Maastricht University, Maastricht, the Netherlands
[b] The Brain and Mind Institute, University of Western Ontario, 1151 Richmond St. N., London, ON N6A 5B7, Canada
[c] Cochlear Benelux NV, Mechelen Campus - Industrie Noord, Schaliënhoevedreef 20, Building I, Mechelen B-2800, Belgium
[d] Department of Ear Nose and Throat/Head and Neck Surgery, Maastricht University Medical Center, Maastricht, the Netherlands
[e] Department of Ear Nose and Throat/Head and Neck Surgery, Zuyderland Medical Center, Sittard/Heerlen, the Netherlands
[f] Department of Ear Nose and Throat /Audiology, School for Mental Health and Neuroscience (MHENS), Maastricht University Medical Center, Maastricht, the Netherlands
[g] Maastricht Centre for Systems Biology, Maastricht University, Maastricht, the Netherlands
[h] UMC Utrecht, department of Otolaryngology- Head and Neck Surgery, UMC Utrecht Brain Center, Utrecht, the Netherlands
[i] Center for Magnetic Resonance Research, University of Minnesota, Minneapolis, MN, United States

ARTICLE INFO

Keywords:
Tinnitus
Ultra-high field MRI
Tonotopic maps
Auditory pathway
Resting-state connectivity

ABSTRACT

Tinnitus is a clinical condition defined by hearing a sound in the absence of an objective source. Early experiments in animal models have suggested that tinnitus stems from an alteration of processing in the auditory system. However, translating these results to humans has proven challenging. One limiting factor has been the insufficient spatial resolution of non-invasive measurement techniques to investigate responses in subcortical auditory nuclei, like the inferior colliculus and the medial geniculate body (MGB). Here we employed ultra-high field functional magnetic resonance imaging (UHF-fMRI) at 7 Tesla to investigate the frequency-specific processing in sub-cortical and cortical regions in a cohort of six tinnitus patients and six hearing loss matched controls. We used task-based fMRI to perform tonotopic mapping and compared the magnitude and tuning of frequency-specific responses between the two groups. Additionally, we used resting-state fMRI to investigate the functional connectivity. Our results indicate frequency-unspecific reductions in the selectivity of frequency tuning that start at the level of the MGB and continue in the auditory cortex, as well as reduced thalamocortical and cortico-cortical connectivity with tinnitus. These findings suggest that tinnitus may be associated with reduced inhibition in the auditory pathway, potentially leading to increased neural noise and reduced functional connectivity. Moreover, these results indicate the relevance of high spatial resolution UHF-fMRI for the investigation of the role of sub-cortical auditory regions in tinnitus.

1. Introduction

Tinnitus is a common hearing disorder characterized by hearing a 'buzzing' or 'ringing' sound in the absence of an external source, and affects approximately 10 to 15% of the general population (McCormack et al., 2014; van Zwieten et al., 2016; Heller et al., 2003). Tinnitus can be experienced temporarily as a result of sound exposure (for instance after a musical concert), but in a subset of cases tinnitus becomes chronic and can lead to a dramatic decrease in the quality of life (Beebe Palumbo et al., 2015). While the origin of subjective tinnitus is believed to stem from peripheral damage (Eggermont and Roberts, 2012), the central auditory mechanisms that underlie the persistent experience of tinnitus are not fully understood.

A number of theories on the neurobiology of tinnitus have been proposed. The auditory pathway contains an orderly organization of neuronal preferred sound frequencies, referred to as tonotopy. The map reorganisation model (Birbaumer et al., 1997; Rauschecker, 1999) proposes that tonotopic organization is modified after peripheral damage. Specifically, it proposes that responses in frequency channels bordering the deafferented ones (i.e. those affected by peripheral damage), now receive inputs from the affected channels, which leads to local tonotopic map expansion and underlies the subjective tinnitus experience (Muhlnickel et al., 2002). An alternative explanation suggests that tinnitus-responsive regions do not necessarily expand, but

* Corresponding author at: Federico De Martino, Oxfordlaan 55, Maastricht 6229 EV, the Netherlands.
E-mail address: f.demartino@maastrichtuniversity.nl (F. De Martino).

https://doi.org/10.1016/j.nicl.2020.102166
Received 30 September 2019; Received in revised form 12 December 2019; Accepted 9 January 2020
Available online 11 January 2020
2213-1582/ © 2020 The Authors. Published by Elsevier Inc. This is an open access article under the CC BY-NC-ND license (http://creativecommons.org/licenses/BY-NC-ND/4.0/).

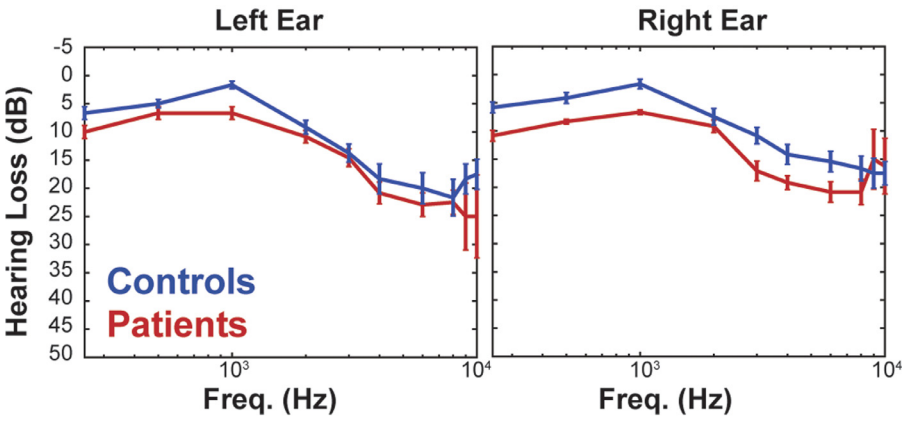

Fig. 1. Audiograms for controls (in blue) and patients (in red) for presented stimuli of different frequencies to the left and right ear. The two groups displayed an absence or only minor hearing loss (< 25 dB) for all presented frequencies. Additionally, the patient-control pair hearing never differed by more than 10 dB for any of the presented tone frequencies.(For interpretation of the references to colour in this figure legend, the reader is referred to the web version of this article.)

display hyperactivity even in the absence of sound (Seki and Eggermont, 2003; Schaette and Kempter, 2006; Gu et al., 2010; Dehmel et al., 2012). Several other proposals have focused on the connectivity between subcortical and cortical auditory regions as the root of the tinnitus experience (Llinas et al., 1999; Lanting et al., 2014). While early studies have supported some of these proposals, results from recent attempts to validate these models have produced mixed results (Langers et al., 2012). As a result, it is generally accepted that tinnitus experience is underlined by a central mechanism, yet there is currently no consensus on what this exact mechanism is.

One of the challenges in studying tinnitus is the difficulty in separating the tinnitus percept from other comorbidities, such as the often co-occurring hearing loss and decreased sound tolerance (DST; Jastreboff & Jastreboff, 2015). This distinction is particularly difficult when studying tinnitus in animal models, but also human studies of tinnitus have often failed to adequately control for confounding factors (Gu et al., 2010). In fact, recent studies suggest that after carefully controlling for hearing loss and DST, previously established differences between tinnitus and control groups disappear (Baguley, 2003; Knipper et al., 2013; Chen et al., 2015).

An additional challenge in human studies is the limited spatial resolution of non-invasive measurement techniques. High spatial resolution is necessary in order to examine the frequency-specificity of responses in subcortical auditory structures, such as the medial geniculate body (MGB) and inferior colliculus (IC), which only measure a few cubic millimeters (e.g. the MGB measures $4 \times 5 \times 4.5$ mm^3; Winer, 1984). Functional magnetic resonance imaging (fMRI) at conventional magnetic fields (3T and below) and with conventional spatial resolution ($> 2 \times 2 \times 2$ mm^3) does not allow examining the frequency-specificity of responses in these small structures. In previous research we have shown that the sensitivity afforded by ultra-high field (UHF) magnetic resonance imaging (MRI) at 7T allows mapping responses in small auditory subcortical structures with sufficient resolution to detail their tonotopic organization (De Martino et al., 2013, 2017; Moerel et al., 2015).

The goal of current research was to transfer this approach to a clinical population. Thus, we examined responses and connectivity throughout the auditory pathway in tinnitus patients and controls at high spatial resolution ($1.5 \times 1.5 \times 1.5$ mm^3) with 7T fMRI. We carefully matched for hearing loss between the patient and control group, and excluded patients who reported DST. We tested whether tinnitus patients demonstrate higher fMRI responsivity to tinnitus pitch in regions along the auditory pathway (specifically IC, MGB, and auditory cortex - AC), and whether the tonotopic maps are abnormal in these regions. Additionally, we examined if the connectivity between auditory processing stages is altered in the tinnitus group, and whether this is specific to connections between regions encoding the tinnitus pitch. For this purpose, we employed resting state fMRI, since rest in tinnitus patients captures their ongoing experience of the tinnitus sound. We observed no large-scale change in tonotopic organization in the tinnitus group. However, the patient and control population differed in the responsiveness to non-preferred frequencies as well as functional connectivity between MGB and AC. Our results demonstrate that ultra-high field fMRI is a viable approach for examining patient populations and that this can yield novel insights on the mechanisms underlying tinnitus.

2. Materials and methods

2.1. Participants

Six tinnitus patients, along with matched controls, participated in this experiment (4 females, 2 males per group; mean age tinnitus patients: 45.4 ± 12.4 years). All tinnitus patients experienced unilateral tinnitus (2 in the left, 4 in the right ear) without DST. Controls were matched for age, i.e. there was less than 5 years age difference between tinnitus patient and matched control (mean age 44.8 ± 12.3 years), sex, handedness (all right-handed) and audiometric hearing loss, i.e. there was a Pure Tone Average (PTA) difference of 10 dB or less between tinnitus patient and matched control (Fig. 1). The absence of cochlear dead regions was confirmed in both the tinnitus and control group with the Threshold-Equalizing Noise (TEN) test (Pepler et al., 2014). Patients and matched controls were recruited through the ENT outpatient clinic and Audiological Center, within the Maastricht University Medical Center+ (MUMC+). The experimental procedures were approved by the Medical Research Ethics Committee (MEC) of the Maastricht UMC+ and Maastricht University (approval No. NL:44760.068.13).

2.2. Tinnitus-specific criteria

All patients experienced unilateral chronic (i.e. longer than 6 months), and subjective tinnitus. Any objective causes, i.e. vascular abnormalities, were excluded as part of the standard medical diagnostics. Patients experienced tinnitus pitch at the following frequencies: 205, 2660, 4470, 5600, 6000 and 8000 Hz. We excluded any patient with DST, phonophobia (persistent, unwanted or abnormal fear of sound) and misophonia (dislike of a specific sound). Additional exclusion criteria for both the patient and control groups included 1) hearing loss of Pure Tone over 50 dB HL for both ears (i.e. mean of hearing loss in decibels for 1k, 2k and 4k Hz), 2) a difference in average hearing threshold of more than 10 dB between the right and left ear (see Fig. 1 for the audiograms), and 3) a history of neurological or psychiatric disorder. Tinnitus complaints were additionally characterized using the tinnitus questionnaire (TQ) questionnaire (Meeus et al., 2007), which includes emotional, cognitive, intrusiveness, auditory, and somatosensory subscales.

2.3. Experimental design

During the acquisition of fMRI data, participants passively listened to blocks of loudness-balanced tones centred around 8 logarithmically spaced centre frequencies (CF) in the range of 0.2 – 10 kHz (i.e. 'tonotopic mapping'). In addition to the eight presented CFs, each pair of patient and matched control was presented with blocks in which the CF matched the patient's reported tinnitus percept. Each block included tones with a variation of ± 0.1 octaves around the CF (i.e. each block consisted of three tones centred around the CF). All tones were amplitude-modulated at 8 Hz (modulation depth = 1) and presented within silent gaps between image acquisitions (tone duration = 800 ms). The level of sound stimulation in the scanner was optimized per participant, so that sounds were clearly audible without being too loud (i.e. highest tolerable level). All subjects underwent six functional runs, with each run containing two repetitions of each centre frequency in a randomised order. One of the patients could only complete four functional runs. For this patient, we analysed four runs also in the matched control volunteer. In all participants, we additionally acquired resting state data. During that scan, participants were asked to lie still and fixate on a white cross presented on a black background for ten minutes.

2.4. Image acquisition

Participants underwent scanning in a 7T scanner (Siemens). Anatomical T_1-weighted (T_1w) images were obtained using a magnetisation-prepared rapid acquisition gradient echo (MPRAGE) sequence (voxel size = 0.6 × 0.6 × 0.6 mm; TR = 3100 ms; TI = 1500 ms; TE = 2.52 ms; flip angle = 5°; generalized autocalibrating partially parallel acquisitions [GRAPPA] = 3). Proton density weighted (PDw) images were additionally acquired to correct for field inhomogeneities (Van de Moortele et al., 2009) (voxel size = 0.6 × 0.6 × 0.6 mm; TR = 1140 ms; TE = 2.52 ms; flip angle = 5°; GRAPPA = 3). Additionally, short inversion T_1-weighted images (SI-T_1w) were obtained. These are T1 weighted images with a modified inversion time to null white matter and thereby maximise the grey matter contrast in subcortical structures (Tourdias et al., 2014; TR = 4500 ms; TI = 670 ms; TE = 3.46 ms; flip angle = 4°; GRAPPA = 3).

Gradient-echo echo planar imaging was used to obtain T_2*-weighted functional data. Functional scans with the opposite phase encoding polarities were acquired to correct for geometric distortions (Andersson et al., 2003). For the functional experiment, acquisition parameters were as follows: TR = 2600 ms; TA = 1400 ms; TE = 19 ms; number of slices = 50, GRAPPA acceleration X2, Multi-Band factor = 2; voxel size = 1.5 × 1.5 × 1.5 mm, silent gap = 1200 ms; 8 min per run. The acquisition parameters for the resting state data were: TR = 2000 ms; TE = 19 ms; number of slices = 50, GRAPPA acceleration X2, Multi-Band factor = 2; voxel size = 1.5 × 1.5 × 1.5 mm, no gap; one run per subject of 10 min.

2.5. Data preprocessing

Functional and anatomical images were analysed in BrainVoyager QX (Brain Innovations, Maastricht) and using custom MATLAB scripts. The ratio between anatomical T_1w images and PDw images was computed to obtain unbiased anatomical images (Van de Moortele et al., 2009). The unbiased anatomical data were normalised in Talairach space (Talairach and Tournoux, 1988) and resampled (with sinc interpolation) to a resolution of 0.5 mm isotropic. A surface reconstruction of each individual hemisphere was obtained by segmenting the gray-white matter boundary. For the analyses of the AC, we performed cortex-based alignment and defined a mask of the AC manually per subject on their inflated surface (and when necessary projected this mask back to the volumetric space by considering a volume of −2 to +3 mm away from the surface in a direction following the normal to the surface). For subcortical analyses, we considered the SI-T_1w map that allows to identify, on the basis of the anatomical contrast, both the MGB and the IC. These anatomical data were initially projected to Talairach space using the same transformation applied to the unbiased anatomical data (i.e. T_1w divided PDw). To improve the alignment across participants in the subcortical regions, one individual brain was used as a reference for additional alignment (affine) steps, tailored separately to 1) optimize alignment for the IC and 2) for the MGB. Single subject transformation information to the common IC and MGB derived on the basis of anatomical information were subsequently used to transform the functional data (see below).

Preprocessing of the functional data consisted of slice-scan-time correction (with sinc interpolation), temporal high-pass filtering (removing drifts of four cycles or fewer per run), 3D motion correction (with trilinear/sinc interpolation and aligning each volume to the first volume of functional run 1), and temporal smoothing (two consecutive data points). Geometric distortions were corrected using FSL's distortion correction tool top-up (Andersson et al., 2003; https://fsl.fmrib.ox.ac.uk/fsl/fslwiki/topup) estimating the voxels' displacement based on data collected with the opposite phase encoding polarities. Functional data were co-registered to the anatomical data, and projected to the normalised space. For the cortical analyses the normalized space was the Talairach space, and the images were re-sampled in Talairach at 1 mm isotropic. For the sub-cortical analyses, images where projected to the tailored IC and MGB spaces and re-sampled at 0.5 mm isotropic (following a procedure similar to the one detailed in De Martino et al., 2013; Moerel et al., 2015).

To perform group analyses of hemisphere laterality relative to the tinnitus percept, the hemispheres of the two patients experiencing tinnitus in the left ear, and their matched controls, were flipped. The flipping was performed both on the level of anatomy as well as for the functional responses. Therefore, the hemisphere 'ipsilateral' to the tinnitus percept was the left hemisphere, and the hemisphere 'contralateral' to the tinnitus percept was the right hemisphere.

2.6. Sound-evoked activation

To characterise the extent of sound-evoked activation, we calculated the functional response to the presentation of each CF in each voxel using a General Linear Model (GLM - Friston et al., 1994) with a predictor for each CF used in the tonotopic localiser. Separate analyses were conducted for the cortex (AC) and subcortical structures (MGB and IC). Predictors were convolved with a standard two-gamma haemodynamic response function (HRF), peaking at 6 s after stimulus onset. Follow-up cortical analyses were restricted to cortical voxels which exhibited significant activation at the level of every individual subject ($t => 2$ [contrast all CFs vs. baseline]; $p < 0.05$ uncorrected – i.e. the GLM was conducted separately per subject and voxel selection was based on single subject statistical results). For subcortical analyses, we instead performed a fixed effect group GLM analysis and restricted follow-up analyses to voxels that exhibited significant activation at the group level ($t => 2.7$ [contrast all CFs vs. baseline]; FDR corrected $q = 0.05$). For the subcortical structures (IC and MGB), we additionally created anatomical masks on the basis of the contrast available in the SI-T_1w and these masks were used to additionally restrict the tonotopic maps to the anatomically identified subcortical regions. All the results are presented in the order respecting the feedforward direction of sound propagation from the periphery – first subcortical structures IC and MGB, followed by the AC.

2.7. Tonotopic mapping and tuning

Tonotopic maps were obtained using 'best frequency mapping' (Formisano et al., 2003), whereby we determined, for every voxel, the tone frequency that elicited the highest fMRI response and colour-coded the voxel accordingly (red – low frequency; blue – high frequency). For

each region of interest (IC, MGB, and AC) this analysis was restricted to voxels where the elicited response to sounds was significant, as outlined above. We additionally separated the AC into primary (PAC) and non-primary AC (non-PAC). PAC was defined anatomically as the medial two thirds of Heschl's gyrus as defined in Kim et al. (2000). Sound-evoked responses were quantified by calculating the mean evoked response in regions preferentially responding to each centre frequency separately, as well as the proportion of voxels most responsive to each presented centre frequency. Moreover, to more fully characterise the responsiveness of voxels, we calculated the tuning function of each voxel (i.e. how much it responded to all of the non-preferred frequencies relative to the best frequency).

2.8. Resting-state seed-based connectivity

We included five out of six pairs of patient-controls in the resting-state connectivity analysis. The sixth pair was excluded because the control participant did not complete the full resting state acquisition (interrupting it after 240 of the 300 planned volumes). For each patient-control pair, two 'seed regions' were defined using the tonotopic maps. The first seed region was defined as voxels responding to their individually-defined tinnitus pitch, while the second seed regions consisted of voxels responding to a control frequency (i.e. the frequency the furthest away from the tinnitus pitch in each patient-control pair). We calculated the functional connectivity between the seed region of one auditory region and all of the voxels in the next auditory regionin the auditory hierarchy. Specifically, we examined the functional connectivity between 1) IC and MGB, 2) MGB and primary AC (PAC), 3) PAC and the rest of the AC. The correlation between the timeseries of the seed and target regions was calculated using Pearson correlation (r-values). The obtained r-values were transformed into z-values, which were used to statistically examine the difference between the patient and control group in functional resting-state connectivity strength.

2.9. Statistical quantification

All analyses consisted of examining the effect of group (patients vs. controls). The significance was determined using permutation tests (i.e. switching patient-control label for all possible 2^6 [2^5 in the case of the resting state analysis] combinations) to obtain possible 'null' distributions and assessing how likely the data-observed 'true' value was in the obtained null distribution of permutation values.

3. Results

3.1. Sound-evoked responses do not differ between tinnitus patients and matched controls

We observed significant responses to presented sounds in all regions of interest (IC, MGB and auditory cortex) in every participant. The first question we examined was whether the magnitude of sound-evoked responses differed between tinnitus patients and matched controls. This has been a dominant idea in the literature, suggesting that a hypersensitivity to tinnitus pitch is related to increased activity, (Gu et al., 2010; Knipper et al., 2013). To test for this, we examined the overall response to presented sounds in the IC (Fig. 2A), MGB (Fig. 2B), and the auditory cortex (Fig. 3A), as well as the mean evoked response (beta value) for each region preferring a unique sound frequency. The strength of sound-evoked responses to the tinnitus pitch (shaded area in Figs. 2 and 3) did not differ between the patients and controls across the IC (Fig. 2C – $t = 1.3$, $p_{perm} = 0.09$ and $t = 0.4$, $p_{perm} = 0.34$ in ipsilateral and contralateral regions respectively), MGB (Fig. 2D – $t = 0.9$, $p_{perm} = 0.28$ and $t = 0.9$, $p_{perm} = 0.26$ in ipsilateral and contralateral regions respectively) and auditory cortex (Fig. 3B – $t = 1.02$, $p_{perm} = 0.09$ and $t = 0.7$, $p_{perm} = 0.2$ in ipsilateral and contralateral regions respectively). Also when considering primary AC (PAC) or non PAC separately, the differences remained non-significant (PAC: $t = -0.5$, $p_{perm} = 0.6$ and $t = -0.2$, $p_{perm} = 0.6$; non PAC: $t = 1.1$, $p_{perm} = 0.06$ and $t = 0.8$, $p_{perm} = 0.19$ in ipsilateral and contralateral regions respectively).

3.2. Tinnitus pitch is not over-represented in the tinnitus group

Next, we examined if there were any group differences in tonotopic organization (i.e. the preference of voxels to a specific frequency). Namely, it could be that while the overall response in auditory regions is equal across groups, tinnitus processing is carried out by a different distribution of responses. That is, the processing of the tinnitus pitch could either be performed by 1) fewer and more strongly responsive voxels or 2) more and weakly responsive voxels. Specifically, it has been hypothesized that tinnitus is characterized by an expansion of neurons responsive to tinnitus pitch. Tonotopic maps were successfully reconstructed for both patients and controls at the subcortical level (IC and MGB – Fig. 4A-B), as well as in the cortex (Fig. 5A). In the IC, we observed one low-to-high frequency gradient (red-to-blue) in dorsolateral to ventromedial direction, which was similar in both patient and control groups (Fig. 4A). In MGB (Fig. 4B), we observed a low-high-low frequency preference through the sagittal slices, reflecting a mirror-symmetric tonotopic gradient. This gradient was more prominent in the ipsilateral compared to the contralateral hemisphere in both groups. Finally, tonotopic maps in the auditory cortex also followed the same pattern across groups, with a low frequency region on HG flanked anteriorly (on planum polare) and posteriorly (on planum temporale) by regions preferring higher frequencies (Fig. 5A). Thus, macroscopically the tonotopic maps were similar across the two groups in all auditory regions examined.

We next compared the proportion of voxels tuned to tinnitus frequency across the two groups. No significant difference between the groups was observed in the MGB ($t = 0.9$, $p_{perm} = 0.23$ and $t = 0.4$, $p_{perm} = 0.35$ in ipsilateral and contralateral regions respectively), or in the IC tonotopic maps ($t = 0.5$, $p_{perm} = 0.31$ and $t = 0.81$, $p_{perm} = 0.29$ in ipsilateral and contralateral regions respectively; see Fig. 4C,D). The number of tinnitus-pitched mapped voxels was reduced in the contralateral AC of patients compared to that of controls ($t = 1.34$, $p_{perm} = 0.04$). No significant difference was observed in the ipsilateral AC ($t = 1.4$, $p_{perm} = 0.12$) (see Fig. 5B). When considering primary and non-primary cortical regions separately, this reduction in tinnitus-pitched mapped voxels in patients was present only in the contralateral non-PAC ($t = 1.4$, $p_{perm} = 0.04$), while it was not significant in the ipsilateral non-PAC ($t = 1.5$, $p_{perm} = 0.09$) or PAC bilaterally ($t = 0.3$, $p_{perm} = 0.3$ and $t = 0.2$, $p_{perm} = 0.3$ in ipsilateral and contralateral regions respectively). Overall, our analysis shows no evidence of an over-representation of tinnitus pitch in the patient group at any level of the auditory hierarchy.

3.3. Higher responsivity to non-preferred pitch in the AC and IC of tinnitus patients

While the tonotopic maps consider only the frequency eliciting the highest voxels' response, we examined the response across different (i.e. non-preferred) frequencies by examining the shape of tuning curves in all auditory ROIs. Tuning curves were constructed to indicate the amount of evoked activation to non-preferred frequencies of each voxel relative to the amount of evoked activation for the preferred (i.e. tonotopic-winner) frequency. We observed that IC and AC responses to non-preferred frequencies were higher in tinnitus patients than in controls (Fig. 4E-F, Fig. 5C). This difference was significant as confirmed by a *t*-test combining non-preferred frequencies (4th and 5th frequency away from the best frequency) both for the contralateral IC ($t = 2.6$, $p_{perm} = 0.04$; see Fig. 4E), and the contralateral AC ($t = 2.07$, $p_{perm} = 0.04$; see Fig. 5C). This suggests that in patients with tinnitus, voxels respond less selectively with relatively higher responses to non-

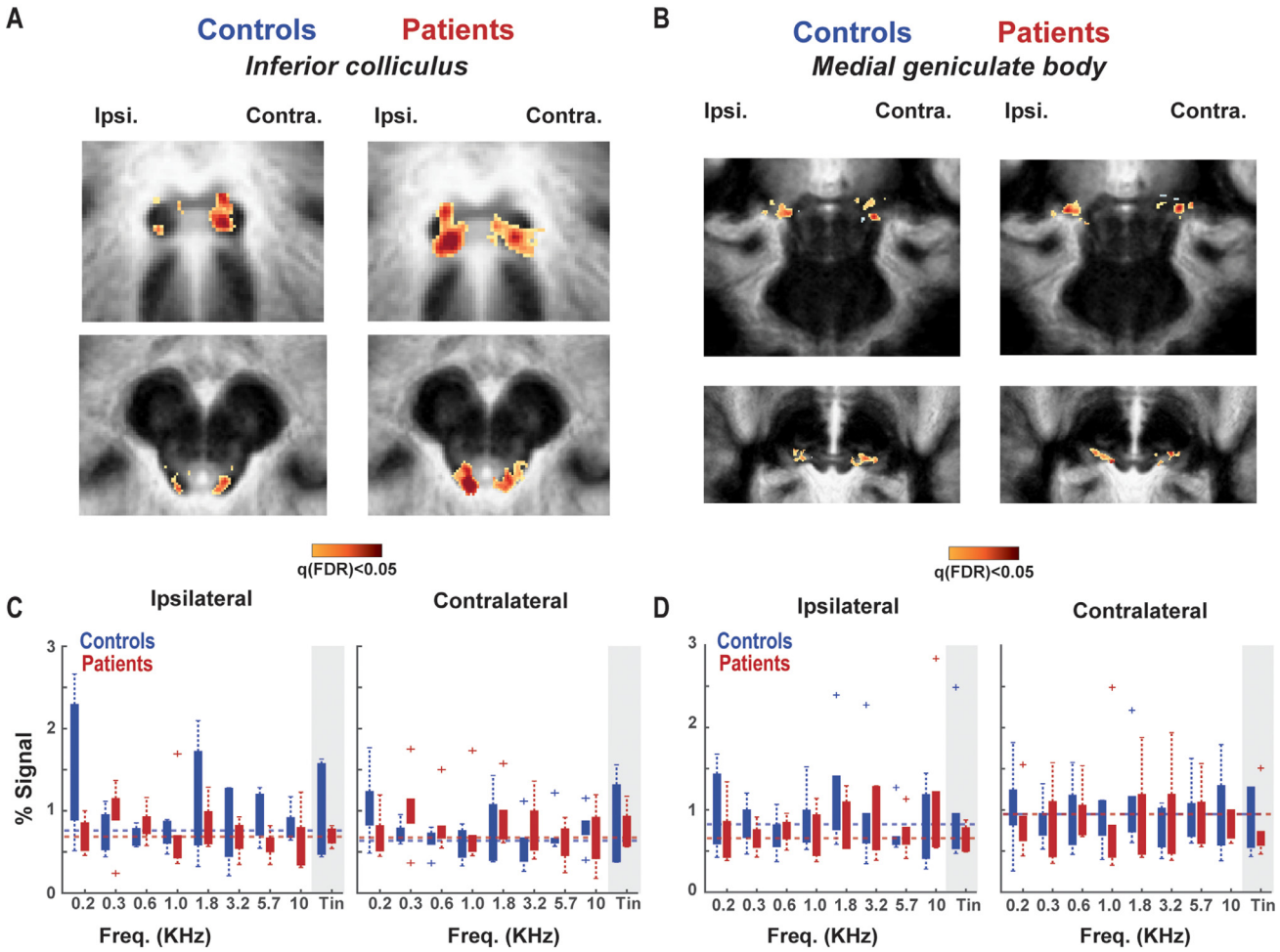

Fig. 2. Sound-evoked response in auditory subcortical structures. A) The mean group sound-evoked response in the **inferior colliculus (IC)**. Voxels with a significant response after FDR correction are displayed in orange-red colours. Group alignment was performed manually to maximise IC overlap across participants (note that the IC alignment is very sharp, while the surroundings are not). **B)** The mean group sound evoked response in the **medial geniculate body (MGB)**. The anatomical alignment was performed manually to maximise the overlap in the MGB. **C)** Activation evoked by the presentation of different sounds in the ipsi- and contralateral IC. **D)** Evoked responses in the MGB to different sounds. There were no significant group differences in activation to tinnitus pitch in ipsilateral or contralateral hemispheres in either IC or MGB.(For interpretation of the references to colour in this figure legend, the reader is referred to the web version of this article.)

preferred frequencies. No significant differences in responsivity between the groups was present in the ipsilateral IC ($t = 1.34$, $p_{perm} = 0.09$), MGB ($t = -0.4$, $p_{perm} = 0.67$; $t = 0.7$, $p_{perm} = 0.26$ in ipsilateral and contralateral regions respectively) and ipsilateral AC ($t = 1.74$, $p_{perm} = 0.06$). When considering primary and non-primary cortical regions separately, the higher responses to non-preferred frequencies for patients were significant in contralateral non-PAC ($t = 2.4$, $p_{perm} = 0.04$), but not in ipsilateral non-PAC ($t = 1.6$, $p_{perm} = 0.09$) or in PAC bilaterally ($t = 0.7$, $p_{perm} = 0.2$ and $t = 1.7$, $p_{perm} = 0.07$ in ipsilateral and contralateral regions respectively). The failure to detect this effect in the PAC can likely be attributed to the loss in power since the number of voxels considered was substantially lower than in other regions of interest.

3.4. Reduced thalamo-cortical resting-state connectivity in tinnitus patients

While several proposals on tinnitus focus on the responsivity of a specific auditory area to the tinnitus pitch, others have suggested the main pathology to lie in the connectivity between auditory regions. Specifically, hypotheses involving abnormal connectivity have focussed on the connection between thalamic and cortical stages of auditory hierarchy (Llinas et al., 1999; Rauschecker et al., 2010). Here we used resting-state connectivity to examine the connectivity between IC and MGB, MGB and primary AC (PAC), and PAC to the rest of AC and tested for differences in connectivity between tinnitus patients and controls. Resting state functional responses might be particularly well-suited for studying tinnitus population sincethe tinnitus experience is present at rest. To tease apart whether any abnormalities in connectivity are specific to tinnitus pitch, or apply in a general manner across all frequencies, we defined seed regions in IC, MGB and PAC to correspond to voxels which responded during the localizer best to the 1) tinnitus pitch or 2) control frequency (the most distant in frequency to the tinnitus pitch).

Starting from the lower levels of the auditory hierarchy, we observed no group difference in the connectivity between the IC and the MGB (Fig. 6). In contrast, connectivity strength between MGB-defined tinnitus pitch voxels and PAC was significantly reduced in tinnitus patients (Fig. 6A). This was the case both when examining the connection between the MGB contralateral to tinnitus percept with contralateral PAC ($t = 1.7$, $p_{perm} = 0.03$) or the connection between the MGB ipsilateral to tinnitus percept to ipsilateral PAC ($t = 1.8$, $p_{perm} = 0.03$; Fig. 6B). No statistical difference was observed between MGB contralateral to tinnitus percept and crossover connection to the ipsilateral PAC ($t = 1.7$, $p_{perm} = 0.06$) or between MGB ipsilateral to tinnitus percept and crossover connection to the contralateral PAC ($t = 1.3$, $p_{perm} = 0.06$; Fig. 6B). Similarly, reduced connectivity was also

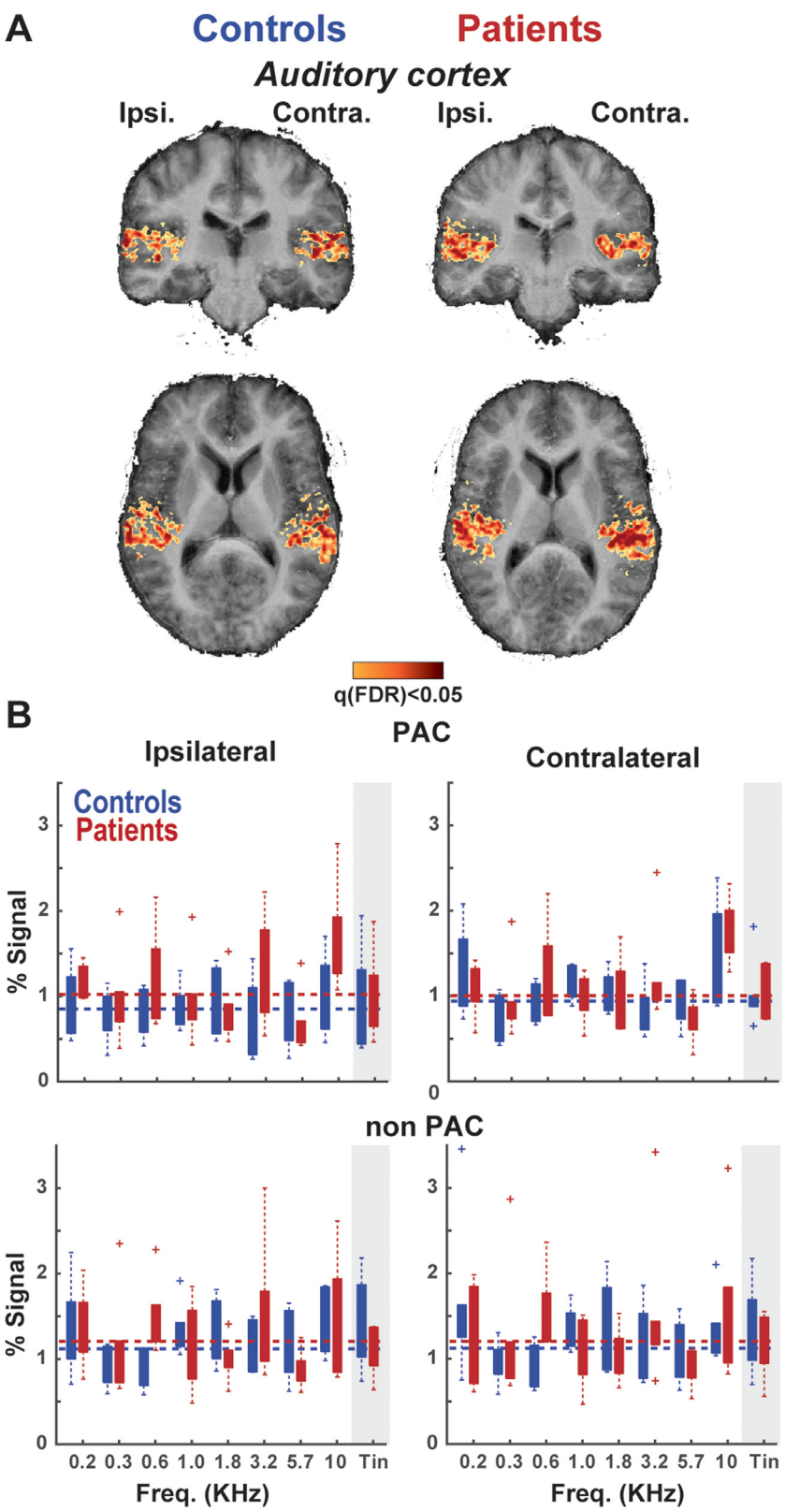

Fig. 3. Sound-evoked response in the auditory cortex. A) The mean group evoked response to sound presentation in the **auditory cortex (AC)**, separately for patient and control groups. Ipsilateral and contralateral denotes the hemisphere ipsi- or contralateral to the experienced tinnitus in patients. Voxels with a significant response after FDR correction are displayed in orange-red colours. Cortical surfaces across individuals were coregistered using cortex-based alignment. **B)** Percent signal change activation to presented sounds of different frequencies, including the tinnitus pitch (gray shade), in the auditory cortex. The dashed line indicates the mean response across all presented frequencies. There was no significant effect of group on elicited activation to tinnitus pitch in ipsilateral or contralateral AC.(For interpretation of the references to colour in this figure legend, the reader is referred to the web version of this article.)

observed between PAC-defined tinnitus pitch voxels and the rest of the AC, both for the contralateral PAC (to contralateral AC: $t = 2.5$ $p_{perm} = 0.03$; crossover ipsilateral AC: $t = 1.8$, $p_{perm} = 0.03$; Fig. 6B), as well as for the ipsilateral PAC (to ipsilateral AC: $t = 1.9$, $p_{perm} = 0.03$; not significant for the contralateral, crossover connection $t = 1.2$, $p_{perm} = 0.06$; Fig. 6B).

Next we examined if these connectivity differences between patients and controls were specific to the tinnitus pitch, or observed also for other sound frequencies. We observed the same profile of connectivity patterns when using the tinnitus-responding voxels or voxels responding best to a control frequency as seed regions for the connectivity analysis. Thus, the observed reduction in connectivity between

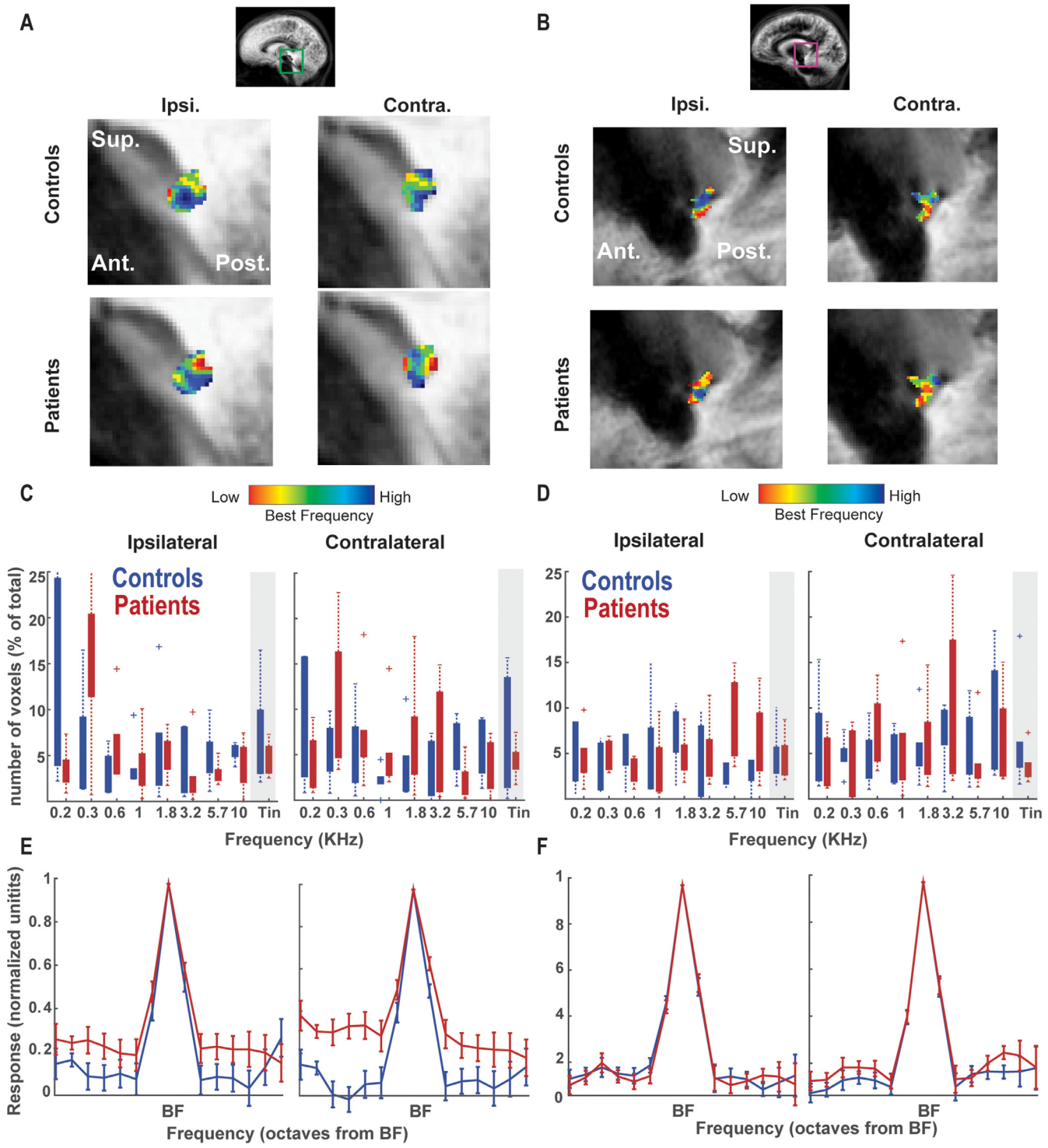

Fig. 4. A) Tonotopy in the **inferior colliculus (IC)**, in tinnitus and control groups. Low frequencies are indicated with red colour, and high frequencies in blue. **B)** Tonotopy in the **medial geniculate body (MGB). C)** Proportion of voxels (y-axis) dedicated to each frequency in the tonotopic map (x-axis) in the IC. Gray shade indicates the tinnitus frequency. **D)** Proportion of voxels responding to different frequencies in the MGB. **E)** Tuning curves in the IC. The center (BF) indicates the best-frequency per voxel, and x-axis is ordered based on the distance from each voxel's BF in octaves. The contralateral IC displayed significantly higher responsivity to-non-preferred frequencies in the patient population than in controls. **F)** Tuning curves in the MGB with no significant group difference in the shape of the responsivity to different frequencies.

thalamic (MGB) and cortical levels (PAC, AC) is not specific to tinnitus pitch.

4. Discussion

We employed the increased spatial resolution achievable with ultra-high field (UHF) MRI at 7T (Yacoub et al., 2002) to explore processing throughout the auditory pathway in a tinnitus population and in

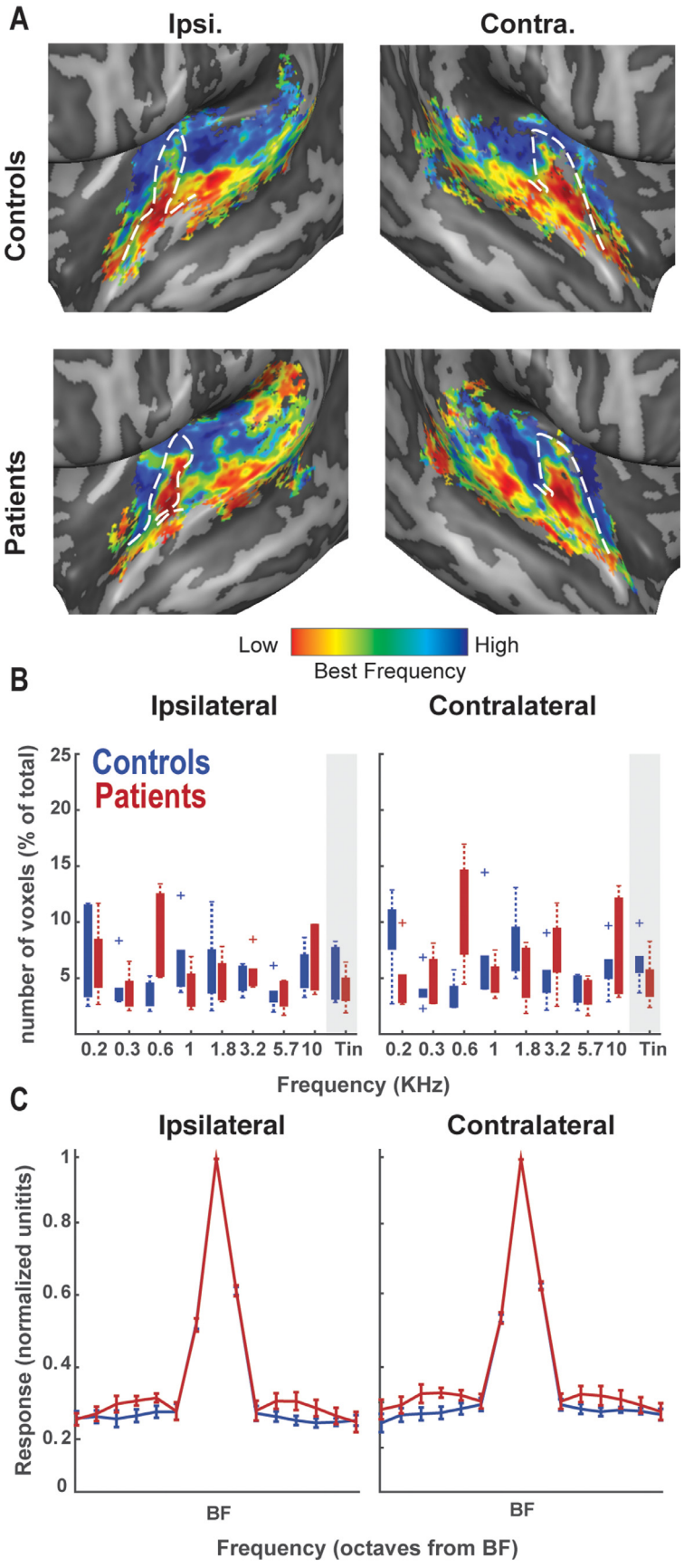

Fig. 5. Tonotopy and tuning curves in the auditory cortex. A) Tonotopic map in the **auditory cortex (AC)** of tinnitus patients and controls. White dashed lines indicate Heschl's gyrus (HG). **B)** Proportion of voxels responding highest to a specific frequency in the tonotopic localizer, or the tinnitus pitch (gray shaded area). On the contralateral site, fewer voxels responded to tinnitus pitch in the patient than in the control group. **C)** Tuning curve depicting the responsivity to non-preferred frequencies across voxels in the auditory cortex in the two groups. The x-axis denotes the frequency presented and its distance from the best-frequency (BF) in octaves. Responses to non-preferred frequencies in the contralateral AC were significantly higher in the patient group.

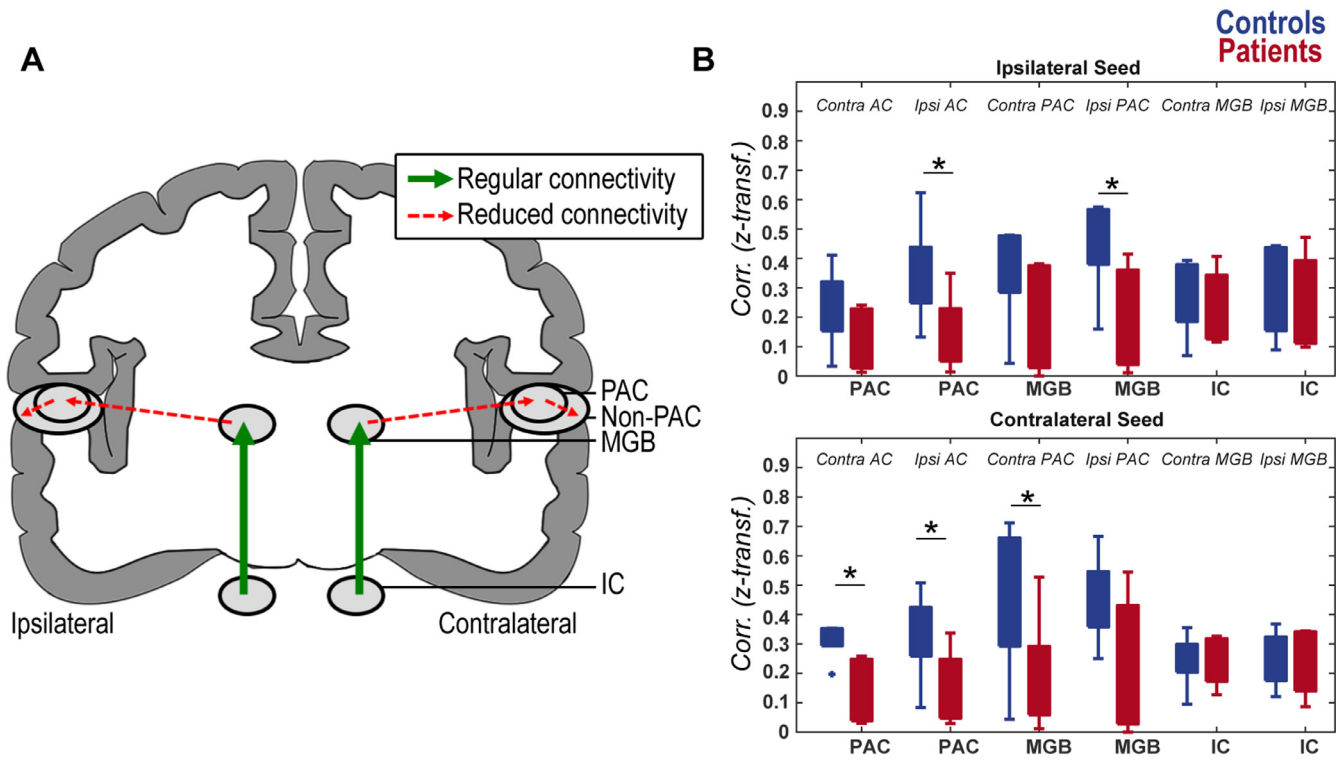

Fig. 6. A) Resting-state connectivity in tinnitus patients, relative to controls. Solid green lines show connections between regions which did not significantly different between groups in resting-state functional connectivity ('Regular connectivity'), while the red dashed lines show significantly reduced resting-state connectivity in tinnitus patients compared to controls ('Reduced connectivity'). The reduced cross-over connectivity between contralateral PAC and ipsilateral non-primary auditory cortex (non-PAC) in patients compared to controls is not shown. **B**) Connectivity strength (measured as z-transformed correlation) in patients (red) and controls (blue) for contralateral (bottom) and ipsilateral (top) seed regions (on the x-axis). The target regions are reported as text in the figures. Significant reduction in connectivity in patients relative to controls is denoted with * ($p_{perm} < 0.05$).(For interpretation of the references to colour in this figure legend, the reader is referred to the web version of this article.)

hearing loss matched controls. We demonstrated the feasibility of examining frequency-specific responses in auditory subcortical regions and in the auditory cortex in this clinical population. While no large-scale changes in tonotopic maps were evident, we observed a modified responsiveness to non-preferred frequencies, as well as differences in functional connectivity between patients and controls. These results should be considered preliminary given our limited sample size, yet suggest that tinnitus may be associated with reduced inhibition, in the auditory pathway, potentially leading to increased neural noise and reduced functional connectivity.

With increasing static magnetic field strength, both signal strength (Uğurbil et al., 2003) and BOLD contrast (Uludağ et al., 2009) increase. The increased signal can be traded for increasing spatial resolution. Due to this effect, UHF MRI provides a potential benefit to those clinical imaging applications where spatial resolution is of key importance (De Martino et al., 2017). One of such examples is the investigation of tinnitus-related changes in brain processing, since auditory subcortical nuclei are small and consist of functionally distinct subfields. Moreover, since processing throughout the auditory pathway is organized in a tonotopic (i.e. frequency-specific) manner and tinnitus-induced changes may be restricted to frequency channels matching the perceived tinnitus pitch, this puts a further demand on the required spatial resolution of the acquired data. However, the application of UHF MRI to patient populations brings concerns that include subject motion and fatigue (Trattnig et al., 2018), both factors which can lower the quality of data. Our results showed that participants were not only able to complete the scans, as none of the patients dropped out partway through the experiment, but that data quality was comparable to what observed in previous experiments performed on young healthy adults. Our study therefore provides a paradigm which can be used to further investigate changes in brain processing with tinnitus at a high spatial resolution, and to extend such studies to include other small structures that have been implicated in tinnitus pathology, such as the thalamic reticular nucleus (TRN; Rauschecker et al., 2010; Leaver et al., 2011) and amygdala (Elgoyhen et al., 2012; D. et al., 2014; Sedley et al., 2015).

In our participant sample, we did not observe evidence for an overall difference in responsiveness to sounds between patients and controls at any level of the auditory pathway, nor a difference in response to the tinnitus pitch. This result contradicts several previous human neuroimaging studies which reported cortical and subcortical hyperactivity to sounds with tinnitus (Lanting et al., 2008; Leaver et al., 2011; Melcher et al., 2017), and interpreted this hyperactivity to be the neural correlate of the experience of subjective tinnitus, possibly stemming from an increased central gain in response to hearing loss. While we cannot exclude that our null result is due to our limited sample size, an explanation for this finding may also originate in the manner by which participants were selected. Namely, in our study we carefully controlled for DST and can therefore be confident that the observed effects are due to tinnitus in the absence of DST. This lack of DST may explain conflicting findings between our current and previous human neuroimaging results as recent findings in animal models showed that DST, not tinnitus, results from increased central gain (Knipper et al., 2013; Rüttiger et al., 2013; Zeng, 2013).

Yet, there are also reports of increased sound responsivity to tinnitus, after accounting for DST. Report by Gu et al. (2010) carefully stratified participants based on DST – while increased sound responsivity in IC and MGB disappeared after accounting for DST, the AC still displayed higher responses in patients with tinnitus. There are several reasons which could contribute to a discrepancy between those

findings and results presented here. First of all, Gu et al. (2010) used a broadband noise stimulus, while we presented amplitude-modulated tones of varying frequencies. This allowed us to dissect sound-evoked responses into their preferred (tonotopy) and un-preferred (tuning curves) parts. Therefore, it is possible that some of Gu et al. (2010) observations were carried by reduced inhibition to non-preferred stimuli, which we observed for contralateral AC (and also IC). Differences in IC might be due to our increased spatial resolution, which possible increased our sensitivity to detect tuning curve abnormalities. Additionally, the two studies differed in the level of stimulus presentation – with Gu et al. (2010) varying sound intensity parametrically, and us presenting the maximum tolerable level of sounds. Gu et al. (2010)'s results could thus reflect perception of louder tones, which was controlled for in our experiment. To clarify the discrepancy, we suggest future studies include both controlled level of stimulus presentation, as well as maximum tolerable level. Last, it is possible that other factors left uncontrolled for (e.g. dietary / caffeine intake; Laurienti et al., 2002) influenced the BOLD response in our study, thereby masking an existing group difference between patients and controls. However, we think such generic factors are unlikely to influence the auditory system in a frequency-specific fashion, but could have possibly influenced the overall sound-evoked response.

Instead of focusing on overall evoked responses to sounds, which can be difficult to interpret, we next dissected overall responses into preferred stimuli and un-preferred stimuli. We first examined possible group differences in the responses to preferred-stimuli, i.e. tonotopic maps, throughout the auditory pathway. Tonotopic maps in the IC and auditory cortex were in accordance with previous reports in a non-clinical population (Da Costa et al., 2011), and indistinguishable between patient and control groups. In the ipsilateral MGB we observed a low-high-low frequency preference in line with previous reports (Moerel et al., 2015) in both the control and patient groups. However, the tonotopic pattern in the contralateral MGB of both groups was not straightforward to interpret. As a similar result was observed across groups, we suggest that the origin of this atypical tonotopic pattern is methodological. The spatial resolution of the collected functional data may have been insufficient to achieve a detailed tonotopic mapping of MGB. For future tonotopic studies of the auditory thalamus, we therefore recommend a spatial resolution of 1.1 mm isotropic (following Moerel et al., 2015). Moreover, while alignment across subjects was performed with great care for each subcortical region, possible misalignments may have added noise to group tonotopic maps. Non-linear tools might instead be preferable to align the brainstem in future endeavours (Sitek et al., 2019).

The lack of differences in tonotopic maps between patients and control may come as a surprise since previous proposals related the tinnitus percept to an expansion of neurons responsive to tinnitus pitch (Muhlnickel et al., 2002). One possibility for this observation is the insufficient statistical power of our study or spatial resolution employed. However, early reports on tonotopic map plasticity in animal models (Rajan and Irvine, 1998; Noreña et al., 2006; Stolzberg et al., 2011) and large-scale map rearrangement in human tinnitus patients (Muhlnickel et al., 2002), were later not replicated by others (Langers et al., 2012; Ghazaleh et al., 2017). In fact, it has been suggested that tonotopic map changes observed in early studies may have been related to hearing loss rather than tinnitus (Eggermont, 2016), and our results support that conclusion. While we observed no large-scale tonotopic differences, we did find an under-representation of tinnitus frequency in the auditory cortex contralateral to the tinnitus percept. We suggest that this finding may have its origin in neural adaptation (Grill-Spector et al., 2006) or a saturation of the BOLD response in those parts of the tonotopic map that match the tinnitus frequency, due to the continuous perception of this frequency by patients.

When we next examined the full frequency tuning curves of voxels, we observed stronger responses to the non-preferred frequencies in tinnitus patients compared to controls. This effect was qualitatively present throughout the auditory pathway, but only significant in the contralateral auditory cortex and the IC. The higher responsivity to non-preferred frequencies suggests reduced inhibition in tinnitus patients, which is in accordance with findings of reduced GABAergic inhibition in animal studies of tinnitus (Middleton et al., 2011; Brozoski et al., 2012; Llano et al., 2012) as well as human patients (Sedley et al., 2015). Importantly, as we failed to observe an increase in sound-driven responses, the higher responsivity to non-preferred frequencies may be non-functional and instead interpreted as an increase in neural noise with tinnitus (Zeng, 2013).

Finally, we observed differences in resting-state functional connectivity between tinnitus patients and controls. While resting state scans are typically defined as task-free, it is important to acknowledge that during rest participants passively listen to noisy background of EPI cycle acquisition. Still, taking into account that the rest state involves passive listening, the two groups still differ critically in their experience of 'rest', which involves hearing the tinnitus percept for the patients. No differences were seen in the connection between IC and MGB, but reduced functional connectivity in tinnitus patients was observed between the MGB and PAC, as well as in the connectivity from PAC to the rest of the auditory cortex. The reduction in functional connectivity was not specific to the tinnitus frequency, but was also observed for seeds consisting of voxels responding to a control (non-tinnitus) frequency. This finding is in accordance with previous studies (Lanting et al., 2008; Kim et al., 2012; Hofmeier et al., 2018; Boyen et al., 2014; but see also Davies et al., 2014), and suggests a generalized modification in connectivity that originates at the level of the MGB and is preserved throughout the auditory cortex. Previous studies have suggested that the ventral MGB may play a crucial role in the generation of tinnitus pathology. Specifically, the thalamocortical dysrhythmia (TCD) hypothesis suggests that tinnitus occurs due to an MGB firing mode-switch resulting from MGB hyperpolarization (Llinas et al., 1999). Instead, the noise cancellation hypothesis (Rauschecker et al., 2010; Leaver et al., 2011) proposes that the tinnitus percept results from a thalamic reticular nucleus (TRN) based release of MGB inhibition. Our results are in accordance with the idea of a central role for the MGB in tinnitus pathology, but do not allow favouring one of these two hypotheses over the other.

5. Conclusion

In summary, we demonstrated the feasibility of translating a high spatial resolution UHF imaging paradigm used in healthy volunteers to study tinnitus. Our preliminary results suggest that tinnitus is associated with a reduced inhibition in the auditory pathway, leading to increased noise and reduced functional connectivity starting at the level of the MGB. Given our limited sample size, these findings require replication in a larger population. Future investigations may extend our paradigm to delineate different aspects of tinnitus pathology (hearing loss, tinnitus percept, DST) using several levels of control groups (healthy adults, hearing loss, hearing loss + DST etc.). Such comprehensive examination will provide novel insights about the involvement of both auditory and higher order brain regions in tinnitus pathology.

Funding

F.D.M. and O.F.G. were supported by NWO VIDI grant 864–13–012, M.M. was supported by NWO VENI grant number 451–15–012, E.B. was supported by Ad Futura Programme of the Slovenian Human Resources and Scholarship Fund. This research has been made possible with the support of the Dutch Province of Limburg.

Declaration of Competing Interest

The content of this article does not reflect the opinion of Cochlear Ltd. and Cochlear Ltd. did not affect the content of this article. The

creation of this article is not financed by Cochlear Ltd.

References

Andersson, J.L.R., Skare, S., Ashburner, J., 2003. How to correct susceptibility distortions in spin-echo echo-planar images: application to diffusion tensor imaging. Neuroimage 20, 870–888. Available at. http://www.ncbi.nlm.nih.gov/pubmed/14568458.

Baguley, D.M., 2003. Hyperacusis. J. R. Soc. Med. 96, 16–19.

Beebe Palumbo, D., Joos, K., De Ridder, D., Vanneste, S., 2015. The management and outcomes of pharmacological treatments for tinnitus. Curr. Neuropharmacol. 13, 692–700.

Birbaumer, N., Lutzenberger, W., Montoya, P., Larbig, W., Unertl, K., Töpfner, S., Grodd, W., Taub, E., Flor, H., 1997. Effects of regional anesthesia on phantom limb pain are mirrored in changes in cortical reorganization. J. Neurosci. 17, 5503–5508. Available at. http://www.ncbi.nlm.nih.gov/pubmed/9204932.

Boyen, K., de Kleine, E., van Dijk, P., Langers, D.R., 2014. Tinnitus-related dissociation between cortical and subcortical neural activity in humans with mild to moderate sensorineural hearing loss. Hear. Res. 312, 48–59.

Brozoski, T., Odintsov, B., Bauer, C., 2012. Gamma-aminobutyric acid and glutamic acid levels in the auditory pathway of rats with chronic tinnitus: a direct determination using high resolution point-resolved proton magnetic resonance spectroscopy (1H-MRS). Front. Syst. Neurosci. 6, 1–12.

Chen, Y.-C., Li, X., Liu, L., Wang, J., Lu, C.-Q., Yang, M., Jiao, Y., Zang, F.-C., Radziwon, K., Chen, G.-D., Sun, W., Krishnan Muthaiah, V.P., Salvi, R., Teng, G.-J., 2015. Tinnitus and hyperacusis involve hyperactivity and enhanced connectivity in auditory-limbic-arousal-cerebellar network. Elife 4, 1–19.

DR, D., V, S., W, N., L, A., S, W., E, A.B., L, B., 2014. An integrative model of auditory phantom perception: tinnitus as a unified percept of interacting separable subnetworks. Neurosci. Biobehav. Rev. 44, 16–32. Available at. http://www.embase.com/search/results?subaction=viewrecord&from=export&id=L52601299%0Ahttp://dx.doi.org/10.1016/j.neubiorev.2013.03.021.

Da Costa, S., van der Zwaag, W., Marques, J.P., Frackowiak, R.S.J., Clarke, S., Saenz, M., 2011. Human primary auditory cortex follows the shape of Heschl's Gyrus. J. Neurosci. 31, 14067–14075. Available at. http://www.jneurosci.org/cgi/doi/10.1523/JNEUROSCI.2000-11.2011.

Davies, J., Gander, P.E., Andrews, M., Hall, D.A., 2014. Auditory network connectivity in tinnitus patients: a resting-state fMRI study. Int. J. Audiol. 53, 192–198.

De Martino, F., Moerel, M., Van De Moortele, P.F., Ugurbil, K., Goebel, R., Yacoub, E., Formisano, E., 2013. Spatial organization of frequency preference and selectivity in the human inferior colliculus. Nat. Commun. 4, 1–8.

De Martino, F., Yacoub, E., Kemper, V., Moerel, M., Uludag, K., De Weerd, P., Ugurbil, K., Goebel, R., Formisano, E., 2017. The impact of ultra-high field MRI on cognitive and computational neuroimaging. Neuroimage 1–17. Available at. http://linkinghub.elsevier.com/retrieve/pii/S1053811917302860.

Dehmel, S., Pradhan, S., Koehler, S., Bledsoe, S., Shore, S., 2012. Noise overexposure alters long-term somatosensory-auditory processing in the dorsal cochlear nucleus–possible basis for tinnitus-related hyperactivity? J. Neurosci. 32, 1660–1671.

Eggermont, J.J., 2016. Can animal models contribute to understanding tinnitus heterogeneity in humans? Front. Aging Neurosci. 8, 1–9.

Eggermont, J.J., Roberts, L.E., 2012. The neuroscience of tinnitus: understanding abnormal and normal auditory perception. Front. Syst. Neurosci. 6, 1–4. Available at. http://journal.frontiersin.org/article/10.3389/fnsys.2012.00053/abstract.

Elgoyhen, A.B., Langguth, B., Vanneste, S., De Ridder, D., 2012. Tinnitus: network pathophysiology-network pharmacology. Front. Syst. Neurosci. 6, 1–12.

Friston, K.J., Worsley, K.J., Poline, J.-P.B., Frith, C.D., Frackowiak, R.S.J., Holmes, aP, Worsley, K.J., Poline, J.-P.B., Frith, C.D., Frackowiak, R.S.J., 1994. Statistical parametric maps in functional imaging: a general linear approach. Hum. Brain Mapp. 2, 189–210. Available at. http://doi.wiley.com/10.1002/hbm.460020402.

Ghazaleh, N., Der, Z.W.V., Clarke, S., 2017. High-Resolution fMRI of auditory cortical map changes in unilateral hearing loss and tinnitus. Brain Topogr. 30, 685–697.

Grill-Spector, K., Henson, R., Martin, A., 2006. Repetition and the brain: neural models of stimulus-specific effects. Trends Cogn. Sci. 10, 14–23.

Gu, J.W., Halpin, C.F., Nam, E.-C., Levine, R.A., Melcher, J.R., 2010. Tinnitus, diminished sound-level tolerance, and elevated auditory activity in humans with clinically normal hearing sensitivity. J. Neurophysiol. 104, 3361–3370. Available at. http://www.physiology.org/doi/10.1152/jn.00226.2010.

Hofmeier, B., Wolpert, S., Aldamer, E.S., Walter, M., Thiericke, J., Braun, C., Zelle, D., Rüttiger, L., Klose, U., Knipper, M., 2018. Reduced sound-evoked and resting-state bold fMRI connectivity in tinnitus. NeuroImage Clin. 20, 637–649.

Kim, J.-J., Crespo-Facorro, B., Andreasen, N.C., O'Leary, D.S., Zhang, B., Harris, G., Magnotta, V.A., 2000. An MRI-Based parcellation method for the temporal lobe. Neuroimage 11, 271–288.

Kim, J.Y., Kim, Y.H., Lee, S., Seo, J.H., Song, H.J., Cho, J.H., Chang, Y., 2012. Alteration of functional connectivity in tinnitus brain revealed by resting-state fMRI?: a pilot study. Int. J. Audiol. 51, 413–417.

Knipper, M., Van Dijk, P., Nunes, I., Rüttiger, L., Zimmermann, U., 2013. Advances in the neurobiology of hearing disorders: recent developments regarding the basis of tinnitus and hyperacusis. Prog. Neurobiol. 111, 17–33.

Langers, D.R.M., de Kleine, E., van Dijk, P., 2012. Tinnitus does not require macroscopic tonotopic map reorganization. Front. Syst. Neurosci. 6, 1–15.

Lanting, C.P., De Kleine, E., Bartels, H., Van Dijk, P., 2008. Functional imaging of unilateral tinnitus using fMRI. Acta Otolaryngol. 128, 415–421.

Lanting, C.P., De Kleine, E., Langers, D.R.M., Van Dijk, P., 2014. Unilateral tinnitus: changes in connectivity and response lateralization measured with fMRI. PLoS ONE 9.

Laurienti, P.J., Field, A.S., Burdette, J.H., Maldjian, J.A., Yen, Y.F., Moody, D.M., 2002. Dietary caffeine consumption modulates fMRI measures. Neuroimage 17 (2), 751–757.

Leaver, A.M., Renier, L., Chevillet, M.A., Morgan, S., Kim, H.J., Rauschecker, J.P., 2011. Dysregulation of limbic and auditory networks in tinnitus. Neuron 69, 33–43. Available at. http://dx.doi.org/10.1016/j.neuron.2010.12.002.

Llano, D.A., Turner, J., Caspary, D.M., 2012. Diminished cortical inhibition in an aging mouse model of chronic tinnitus. J. Neurosci. 32, 16141–16148.

Llinas, R.R., Ribary, U., Jeanmonod, D., Kronberg, E., Mitra, P.P., 1999. Thalamocortical dysrhythmia: a neurological and neuropsychiatric syndrome characterized by magnetoencephalography. Proc. Natl. Acad. Sci. 96, 15222–15227. Available at. http://www.pnas.org/cgi/doi/10.1073/pnas.96.26.15222.

McCormack, A., Edmondson-Jones, M., Fortnum, H., Dawes, P., Middleton, H., Munro, K.J., Moore, D.R., 2014. The prevalence of tinnitus and the relationship with neuroticism in a middle-aged UK population. J. Psychosom. Res. 76, 56–60.

Melcher, J.R., Sigalovsky, I.S., Guinan, J.J., Levine, R.A., 2017. Lateralized tinnitus studied with functional magnetic resonance imaging: abnormal inferior colliculus activation. J. Neurophysiol. 83, 1058–1072.

Middleton, J.W., Kiritani, T., Pedersen, C., Turner, J.G., Shepherd, G.M.G., Tzounopoulos, T., 2011. Mice with behavioral evidence of tinnitus exhibit dorsal cochlear nucleus hyperactivity because of decreased GABAergic inhibition. Proc. Natl. Acad. Sci. 108, 7601–7606.

Moerel, M., De Martino, F., Ugurbil, K., Yacoub, E., Formisano, E., 2015. Processing of frequency and location in human subcortical auditory structures. Sci. Rep. 5, 1–15.

Muhlnickel, W., Elbert, T., Taub, E., Flor, H., 2002. Reorganization of auditory cortex in tinnitus. Proc. Natl. Acad. Sci. 95, 10340–10343.

Noreña, A.J., Tomita, M., Eggermont, J.J., 2006. Neural changes in cat auditory cortex after a transient pure-tone trauma. J. Neurophysiol. 90, 2387–2401.

Pepler, A., Munro, K.J., Lewis, K., Kluk, K., Pepler, A., Munro, K.J., Lewis, K., Kluk, K., 2014. Repeatability, agreement, and feasibility of using the threshold equalizing noise test and fast psychophysical tuning curves in a clinical setting repeatability, agreement, and feasibility of using the threshold equalizing noise test and fast psychoph. Int. J. Audiol. 53, 745–752.

Rajan, R., Irvine, D.R., 1998. Neuronal responses across cortical field A1 in plasticity. Audiol. Neurootol. 3168, 123–144.

Rauschecker, J.P., 1999. Auditory cortical plasticity: a comparison with other sensory systems. TINS 22, 74–80.

Rauschecker, J.P., Leaver, A.M., Mühlau, M., 2010. Tuning out the noise: limbic-Auditory interactions in tinnitus. Neuron 66, 819–826.

Richard Sitek K., Faruk Gulban O., Calabrese E., Allan Johnson G., Ghosh S.S., De Martino F. (2019) Mapping the human subcortical auditory system using histology, post mortem MRI and in vivo MRI at 7T. Available at: http://dx.doi.org/10.1101/568139.

Rüttiger, L., Singer, W., Panford-Walsh, R., Matsumoto, M., Lee, S.C., Zuccotti, A., Zimmermann, U., Jaumann, M., Rohbock, K., Xiong, H., Knipper, M., 2013. The reduced cochlear output and the failure to adapt the central auditory response causes tinnitus in noise exposed rats. PLoS ONE 8, 1–11.

Schaette, R., Kempter, R., 2006. Development of tinnitus-related neuronal hyperactivity through homeostatic plasticity after hearing loss: a computational model. Eur. J. Neurosci. 23, 3124–3138.

Sedley, W., Gander, P.E., Kumar, S., Oya, H., Kovach, C.K., Nourski K, V., Kawasaki, H., Howard, M.A., Griffiths, T.D., 2015. Intracranial mapping of a cortical tinnitus system using residual inhibition. Curr. Biol. 25, 1208–1214.

Seki, S., Eggermont, J.J., 2003. Changes in spontaneous firing rate and neural synchrony in cat primary auditory cortex after localized tone-induced hearing loss. Hear. Res. 180, 28–38.

Stolzberg, D., Chen, G.D., Allman, B.L., Salvi, R.J., 2011. Salicylate-induced peripheral auditory changes and tonotopic reorganization of auditory cortex. Neuroscience 180, 157–164.

Tourdias, T., Saranathan, M., Levesque, I.R., Su, J., Rutt, B.K., 2014. Visualization of intra-thalamic nuclei with optimized white-matter-nulled MPRAGE at 7T. Neuroimage 84, 534–545.

Trattnig, S., Springer, E., Bogner, W., Hangel, G., Strasser, B., Dymerska, B., Cardoso, P.L., Robinson, S.D., 2018. Key clinical benefits of neuroimaging at 7 T. Neuroimage 168, 477–489.

Uğurbil, K., Adriany, G., Andersen, P., Chen, W., Garwood, M., Gruetter, R., Henry, P.G., Kim, S.G., Lieu, H., Tkac, I., Vaughan, T., Van De Moortele, P.F., Yacoub, E., Zhu, X.H., 2003. Ultrahigh field magnetic resonance imaging and spectroscopy. Magn. Reson. Imaging 21, 1263–1281.

Uludağ, K., Müller-Bierl, B., Uğurbil, K., 2009. An integrative model for neuronal activity-induced signal changes for gradient and spin echo functional imaging. Neuroimage 48, 150–165.

Van de Moortele, P.F., Auerbach, E.J., Olman, C., Yacoub, E., Uğurbil, K., Moeller, S., 2009. T1 weighted brain images at 7 Tesla unbiased for proton density, T2 * contrast and RF coil receive B1 sensitivity with simultaneous vessel visualization. Neuroimage 46, 432–446.

Winer, J.A., 1984. The human medial geniculate body. Hear. Res. 15, 225–247.

Yacoub, E., Shmuel, A., Pfeuffer, J., Van De Moortele, P.-F., Adriany, G., Andersen, P., Vaughan, J.T., Merkle, H., Ugurbil, K., Hu, X., 2002. Imaging brain function in humans at 7 Tesla. Magn. Reson. Med. 45, 588–594.

Zeng, F.G., 2013. An active loudness model suggesting tinnitus as increased central noise and hyperacusis as increased nonlinear gain. Hear. Res. 295, 172–179.